

## MIT Open Access Articles

*Water Infiltration in ZSM-5 Zeolites: Effect of Pore Volume and Water Structure*

The MIT Faculty has made this article openly available. **Please share** how this access benefits you. Your story matters.

**Citation:** Maroo, Shalabh C., Tom Humplik, Tahar Laoui, and Evelyn N. Wang. "Water Infiltration in ZSM-5 Zeolites: Effect of Pore Volume and Water Structure." Proceedings of the ASME 2012 Third International Conference on Micro/Nanoscale Heat and Mass Transfer, 3-6 March 3, 2012, Atlanta, Georgia, ASME, 2012. © 2012 by ASME

**As Published:** <http://dx.doi.org/10.1115/MNHMT2012-75322>

**Publisher:** ASME International

**Persistent URL:** <http://hdl.handle.net/1721.1/120001>

**Version:** Final published version: final published article, as it appeared in a journal, conference proceedings, or other formally published context

**Terms of Use:** Article is made available in accordance with the publisher's policy and may be subject to US copyright law. Please refer to the publisher's site for terms of use.



**MNHMT2012-75322**

## **WATER INFILTRATION IN ZSM-5 ZEOLITES: EFFECT OF PORE VOLUME AND WATER STRUCTURE**

<sup>1</sup>#Shalabh C. Maroo, <sup>1</sup>Tom Humpalik, <sup>2</sup>Tahar Laoui & <sup>1</sup>Evelyn N. Wang

<sup>1</sup>Department of Mechanical Engineering, Massachusetts Institute of Technology (MIT), Cambridge MA 02139

<sup>2</sup>Department of Mechanical Engineering, King Fahd University of Petroleum and Minerals, Dhahran, Saudi Arabia

#presently at Department of Mechanical & Aerospace Engineering, Syracuse University, Syracuse NY 13244

### **ABSTRACT**

This study investigates the infiltration of water in ZSM-5 zeolite crystals via molecular dynamics simulations and experiments. A zeolite nano-crystal is constructed in the simulations and is surrounded by water molecules which enter and saturate the pores. The average number of water molecules per unit cell of the zeolite is determined along with the radial distribution function of water inside the zeolites. A geometric approximation of the zeolite pores and intersections is proposed and verified. Partial charge on the zeolite atoms is found to be a crucial parameter which governs the water infiltration behavior. ZSM-5 zeolite crystals were also synthesized and water infiltration experiments were conducted using an Instron. The simulation and experimental findings are compared and discussed. The understanding gained from these studies will be important for the development of zeolite based reverse osmosis membranes for water desalination.

### **INTRODUCTION**

Zeolites are primarily aluminosilicate minerals with a microstructure composed of 3–8 Å pores. While zeolites were first discovered as naturally occurring crystals, they can be synthesized with controllable size and morphology in a laboratory environment with hydrothermal or microwave synthesis techniques [1]. Crystal morphology and size can be controlled from a few nanometers to hundreds of millimeters by varying synthesis temperature, time

and technique [1]. Properties such as adsorption characteristics, geometry, ion exchange capabilities, and catalytic behavior differ amongst the zeolite crystal family and can be tailored to a specific application by using the correct composition and pore geometry. The combination of high porosity and high active surface area has led to significant zeolite research for catalytic applications. In commercial applications, the most common use for zeolites is as adsorbents during various chemical processes. Recently, researchers have begun to utilize the sub-nanometer pore sizes of zeolites as a medium for gas separation and water desalination [2-4]. Murad and Lin used molecular dynamics simulations to investigate the ion separation of a single ZK-4 type zeolite with 4.4 Å diameter pores in a NaCl-water solution [5, 6]. Although the flux of water could not be determined from these simulations, Murad and Lin hypothesized that a defect free zeolite membrane could reject 100% of the salt ions since the solvated ions were too large (~7.5 Å) to pass through the pores. However, experimental membranes have yet to achieve high salt rejection primarily due to fabrication difficulties. Researchers have also recently investigated the effects of confinement on water infiltration and transport in various zeolites [7-9]. Specifically, researchers have investigated the effects of modifying various simulation parameters such as the force field, defect density and water model in an attempt to correlate experimental adsorption and infiltration isotherms with simulation results, principally with ZSM-5 zeolites [10-12]. ZSM-5 zeolites are comprised of straight pores, zig-zag pores and intersections, as shown in Fig. 1.

However, as shown in Table 1, the variation in total pore volume of ZSM-5 type zeolites found in literature makes it challenging to determine the validity of past simulations, especially in those simulations that use the total pore volume as a constraint to fit the data to experimental results.

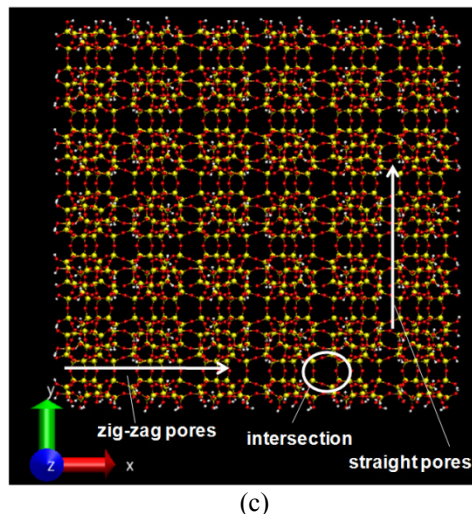
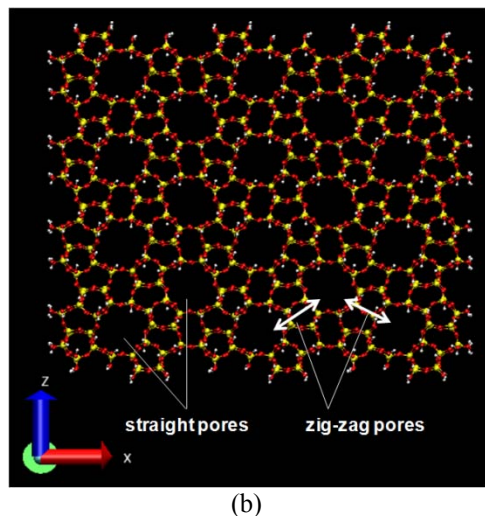
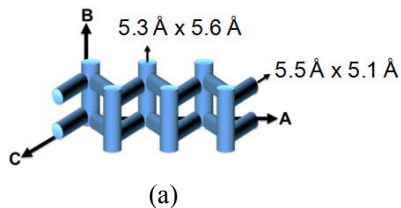


Figure 1: (a) Sketch of ZSM-5 zeolite. Molecular pore structure of ZSM-5 zeolite in (b) x-z plane, and (c) x-y plane. Yellow and red colored atoms denote Si and O, respectively.

Table 1. Variation in experimental and simulated pore volume of ZSM-5 zeolites. Note that a star (\*) denotes the value is from simulations.

Pore Volume (cm <sup>3</sup> /g)	Author
0.186	Trzpit <i>et al.</i> [11]
0.203	Eroshenko <i>et al.</i> [13]
0.11	Hsu <i>et al.</i> [14]
0.28	Zhao <i>et al.</i> [15]
0.11-0.12	Babeva <i>et al.</i> [16]
0.22	Lu <i>et al.</i> [17]
0.192*	Desbien <i>et al.</i> [18]

The primary method to determine the pore volume of zeolites is to perform a BET analysis using nitrogen as the probe fluid and obtain an adsorption isotherm; however, it is unclear if the volume that nitrogen molecules occupy is the same volume that water molecules would occupy, especially at these sub-nanometer scales. Additionally, various other parameters such as defect density, crystal size, and adsorbed gas molecules could affect the measured pore volume as well. Therefore, a more rigorous experimental and modeling approach is needed to determine the total ZSM-5 pore volume for water. A better evaluation of the applicability of zeolites in water desalination can be obtained by relating experimental and simulation results to create a more accurate model of water transport inside zeolites, which is the focus of this study.

## SIMULATION MODEL

Water infiltration in ZSM-5 zeolites was modeled using the molecular dynamics simulation package GROMACS [19]. A zeolite crystal was constructed based on the database of zeolite structures [20], and positioned in the computational domain such that the straight pores were parallel to the z-axis. The crystal had dimensions: 4.0180 nm × 3.9426 nm × 6.0980 nm (i.e. 2 u.c. × 3 u.c. × 3 u.c.; based on the defined size of one unit cell, u.c., of ZSM-5 zeolite). The computational domain boundaries were periodic in nature. The x- and y- dimensions of the domain were equal to that of the zeolite crystal in order to model an infinite crystal in the x and y directions. Since hydroxyl groups are generally found on the surface of zeolites [21], hydrogen atoms were added to the dangling oxygen atoms at the z-surface of the crystal to satisfy their electronic valency. The zeolite comprised of 1728 Si, 3552 O and 192 H atoms. The z- dimension of the domain was 96.3422 nm.

The zeolite crystal was surrounded by water in the z-direction as follows: a separate NVT simulation was performed with only water in a domain of  $4.0180 \text{ nm} \times 3.9426 \text{ nm} \times 96.3422 \text{ nm}$ . All boundaries were periodic. SPC water model was used. The number of water molecules was 50869 corresponding to a water density of  $999.9 \text{ kg/m}^3$ . The van-der Waals and Coulomb force interactions were calculated using the Shift model with a cut-off radius of 1 nm. Temperature of the system was maintained at 298 K using the Berendsen thermostat. The simulation was run for 0.5 ns with a timestep of 2 fs. After equilibrium, the zeolite crystal constructed above was placed at the center of the domain by removing water molecules occupying the same space. The overall system, which now consisted of 47387 water molecules, is shown in Fig. 2. A significantly large number of water molecules was used in this work since cavitation was seen, as water entered the pores, in prior simulations with fewer number of water molecules.

Water infiltration in the zeolite crystal was subsequently simulated. Water molecules were

allowed to move beyond time  $t=0$ , while the zeolite atoms were kept fixed at all times. Keeping the zeolite atoms stationary does not alter the transport process of water infiltration since a water molecule is much smaller than the diameter of zeolite pores [22, 23]. Interaction between water molecules and zeolite atoms (*i.e.*, Si, O and H) was modeled using the GROMOS force field. The water molecules were coupled to the berendsen thermostat to maintain the water temperature at 298 K. It has been shown that water infiltration in zeolites, even at very high pressures, does not lead to any significant increase in system temperature [24]. The simulation was run for 2 ns at timesteps of 2 fs. Ideally, as a water molecule enters a zeolite sub-nanometer pore, the proximity of the molecule to the zeolite atoms can induce dipole moments which can alter the charges on specific zeolite and water atoms dynamically. As this is very computationally intensive, constant partial charges of  $\text{Si}=1.1$ ,  $\text{O}=\text{Si}/2=-0.55$  and  $\text{H}=\text{O}/2=0.275$  were assigned, which have also been used in prior literature. The partial charge values highly affect the transport behavior of water in the zeolite pores, which will be shown later in this work.

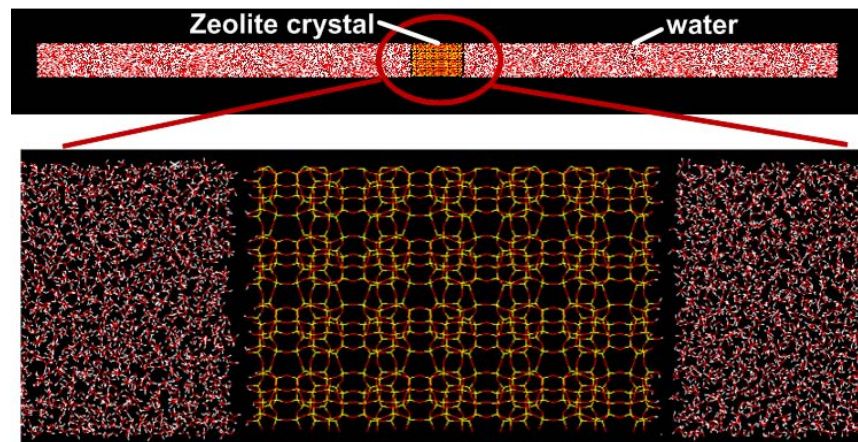


Figure 2: Computation domain initial setup showing zeolite crystal placed at the center of the domain and surrounded by water molecules.

## RESULTS AND DISCUSSION

The results of water infiltration into the zeolite pores were obtained upon completion of the simulation. Figure 3 depicts the zeolite crystal at 2 ns which shows that water completely infiltrates the pores. The amount of water in the zeolite reaches equilibrium at around 1.7 ns. The number of water molecules infiltrated into the zeolite pores is determined over time by averaging over a control volume of 12 u.c. around the center of the zeolite crystal. The

infiltration trend is shown in Fig. 4. In the final 0.3 ns,  $\sim 580$  water molecules are present in the 12 u.c., giving the average value of 48.3 water molecules/u.c.. This average infiltration water mass depends on the water pressure outside the crystal, as no further infiltration occurs when the bulk water pressure equals the net pressure of water inside the zeolite crystal, *i.e.*, an additional simulation performed with initial water density of  $1120 \text{ kg/m}^3$  resulted in a small increase, an average of  $\sim 54.7$  water molecules/u.c..



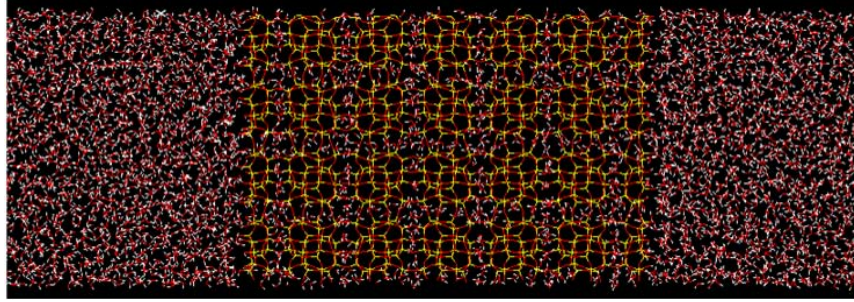


Figure 3: Water infiltration into the pores of the zeolite crystal with molecular dynamics simulations. An average of 48.3 water molecules is present per unit cell of the zeolite at equilibrium in the simulation.

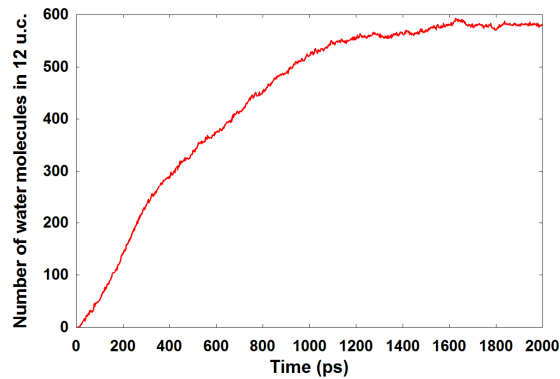


Figure 4: Variation of number of water molecules present in 12 u.c. of the zeolite with time. Amount of water in the zeolite reaches equilibrium at  $\sim 1.7$  ns.

Due to the sub-nanometer sized pores in zeolites (Fig. 1b-c), it becomes difficult to define the boundaries of the straight pores, zig-zag pores and intersections. A small error in the boundary position can result in a significant change in the overall pore volume due to the molecular nature of the pores. This work specifies the pore boundaries of the ZSM-5 zeolites and validates the results. From the exact position of the Si and O atoms within the zeolites, known dimensions of a unit cell, and utilizing the van-der Waals radius of the atoms, the pores are approximated as cylinders and the intersections as cuboids, as shown in Fig. 5. Statistical analysis for an average number of water molecules present in the pores and intersections during final equilibrium results in: 6.5 water molecules/intersection, 3.2 water molecules/zig-zag pores, and 2.5 water molecules/straight pore. As there are four of each in one unit cell, the total number of water molecules per u.c. obtained from this analysis is 48.8, which matches well with the average of 48.3 obtained previously. Thus, the straight pore can be approximated as a cylinder of length 0.445 nm and diameter 0.55 nm, zig-zag pore as cylinder of length 0.547 nm and diameter 0.53 nm, and intersection as cuboid of dimensions 0.7 nm  $\times$  0.73 nm  $\times$  0.62 nm.

Thus, 50% of water present in the zeolite was determined to be located at the intersections. In addition, the maximum pore volume available in a ZSM-5 zeolite was calculated from this analysis and found to be 0.227 cm<sup>3</sup>/g, although the complete volume may not be utilized by water due to its molecule shape and van-der Waal's radius.

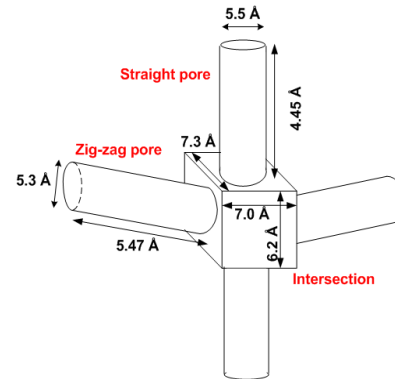


Figure 5: The straight pore, zig-zag pore and intersection of the ZSM-5 crystal is modeled as cylinders and cuboid with the specified dimensions.

The radial distribution function (RDF) of water present in the zeolites is of particular interest as it shows the atomic density varies as a function of the distance from any particular atom. The RDF of atoms B around an atom A is defined by:

$$g_{AB}(r) = \frac{\langle \rho_B(r) \rangle}{\langle \rho_B \rangle_{local}}$$

where  $\rho$  is particle density

The terms in the above equation are depicted in Fig. 6. The RDF of water in zeolites is well-represented by the O atoms, and determined over the final equilibrium period of the simulation. Figure 7 shows the RDF of O-O atoms. Three distinct peaks are observed. The first peak occurring at  $r=0.276$  nm represents the water present at the intersections. The second peak at  $r=0.56$  nm is due to the second shell

of water at the intersection, or more appropriately, at the boundaries of the pores and intersections. The third peak occurs at  $r=1.238$  nm as a result of the water present at the nearest neighboring intersections. For verification, the distance between the first and the third peak is almost equal to the center-to-center distance of nearest neighboring intersections. In addition, superimposition of the RDF of O-O atoms in bulk water shows surprising resemblance between the first peaks. This observation suggests that the molecular structure of water in the immediate proximity of a water molecule in water-saturated zeolite is similar to that of bulk water.

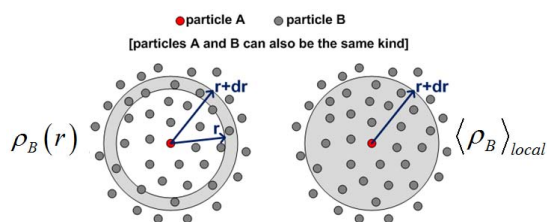


Figure 6: RDF of particles B around particle A.

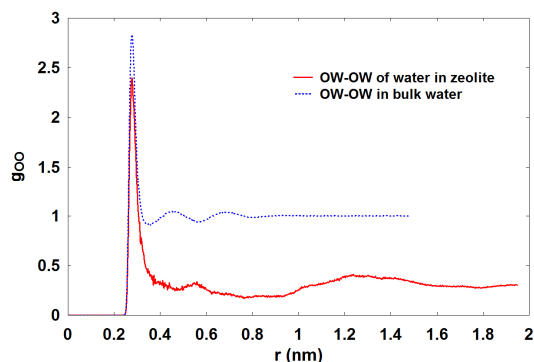


Figure 7: Radial distribution function of water in the zeolite where three distinct peaks are observed. RDF of bulk water is included for comparison.

As mentioned previously, the partial charges on zeolite atoms significantly governs the behavior of water transport in the pores. The results discussed so far have been for the simulation with partial charge of  $\text{Si}=1.1$ , where water molecules were found to easily infiltrate the zeolite pores. In order to study the effect of partial charge on water infiltration, an additional simulation was performed where the charge was changed to  $\text{Si}=3.0$  ( $\text{O}=-1.5$  and  $\text{H}=0.75$ ) while keeping all remaining parameters the same. This change creates a stronger interaction between Si and water's O atom, and as a result water does not infiltrate in the zeolite beyond a certain distance as shown in Fig. 8. An energy analysis on the water molecules depicted as A and B determined that molecule A remained attached on the zeolite due to the stronger interaction than with water. However,

molecule B was still free to move around as B-water interactions were stronger than B-zeolite interactions. Thus, due to the size of the pore which only allows the formation of a single water chain, molecule A being attached prevents further infiltration of water in the zeolite pores. Local molecular equilibrium can exist in these sub-nanometer pores which affect the overall transport behavior of the system. An accurate value of the partial charge in zeolites can be obtained by corroborating simulation results with experiments, which is work ongoing.

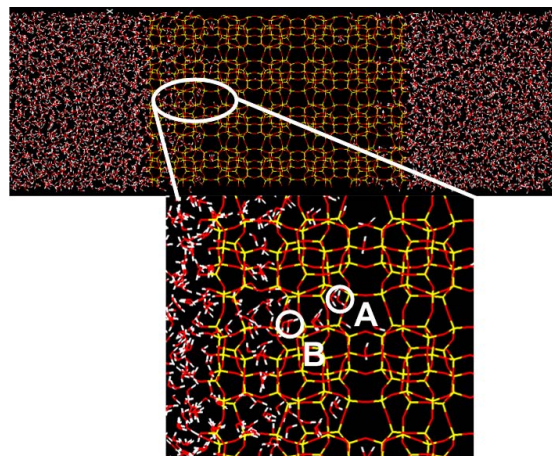


Figure 8: Water infiltration in a zeolite with a partial charge of  $\text{Si}=3.0$ . The effect of the higher partial charge causes water molecules not to infiltrate into the zeolite pores.

### Water Infiltration Experiments

In addition to these simulations, preliminary infiltration experiments were performed. First, ZSM-5 zeolites were synthesized using hydrothermal synthesis techniques. Tetraorthosilicate (TEOS, Sigma Aldrich) was used as the silica source and tetrapropylammonium hydroxide (TPAOH, 20% in  $\text{H}_2\text{O}$ , Sigma Aldrich) was used as the structure-directing agent. The starting solution was a 5:1:100 molar concentration of TPAOH:TEOS: $\text{H}_2\text{O}$ . The solution was stirred and aged overnight. After the mixture homogenized, the solution was vacuum filtered and poured into a PTFE-lined stainless steel autoclave (Parr, Inc.). The autoclave was inserted into an oven held at  $90^\circ\text{C}$  with rotation set at  $\sim 120$  RPM. After 24 hours, the autoclave was quenched to room temperature. The resulting solution was filtered *via* centrifugation and dried at  $50^\circ\text{C}$ . To remove the  $\text{TPA}^+$  ions from the pores, the zeolite powder was calcined at  $550^\circ\text{C}$  for 12 hours. The zeolites have a nominal crystal size of  $\sim 144$  nm  $\pm 20$  nm as seen in the SEM image in Fig. 9.

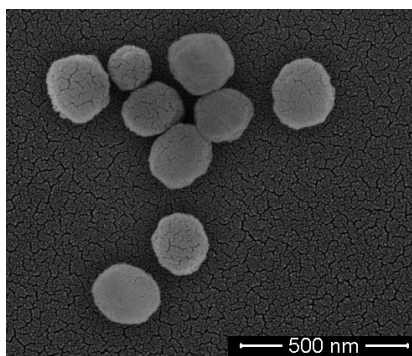


Figure 9: Scanning electron microscope (SEM) image of synthesized ZSM-5 zeolite crystal.

A stainless steel piston-cylinder apparatus capable of handling internal pressure of 200 MPa was fabricated. Approximately 2.5 g of zeolite was mixed into 10 mL of class 2 deionized water (VWR) and transferred into the piston-cylinder apparatus. The test cell was loaded into an Instron 5582 and compressed at a speed of 2 mm/min (corresponding to a volume compression of  $0.253 \text{ cm}^3/\text{min}$ ). The compressibility of the test cell and the Instron were removed by measuring the compression of a control sample consisting of 2.5g of non-calcinated zeolites in 10 mL of water. Figure 10 shows the experimental pressure infiltration data. Maximum water infiltration into the zeolites occurred at an applied pressure of  $\sim 100 \text{ MPa}$ . The intruded volume was found to be  $0.106 \text{ cm}^3/\text{g}$ . This volume was converted to number of water molecules per u.c. by correlating the change in volume per 0.5 MPa with the corresponding density at that pressure. Thus, knowing the amount of zeolite used in the experiment, the average number of water molecules in the zeolite was obtained to be  $\sim 35.5 \pm 1.8$  per u.c..

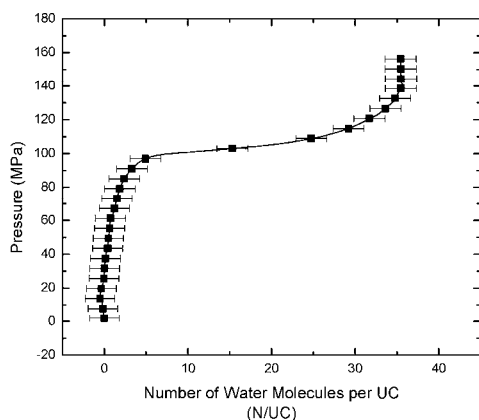


Figure 10: Pressure infiltration curve of water in the synthesized ZSM-5 crystals.

However, this value is lower than that found in simulations and is a part of ongoing research. The reasons of the discrepancy include: 1) presence of pre-adsorbed water, hydroxyl groups and/or gases in experiments, 2) accurate partial charge of zeolites required in simulations, and 3) infiltration length dependency on zeolite crystal size in experiments.

## CONCLUSION

The pore volume and water structure during water infiltration in a ZSM-5 zeolite was investigated using molecular dynamics simulations and experiments. A ZSM-5 zeolite nano-crystal was constructed and surrounded by water molecules to simulate water infiltration. For a silicon partial charge of 1.1 and initial water density of  $999.9 \text{ kg/m}^3$ , an average of  $\sim 48.3$  water molecules were obtained to infiltrate one unit cell of the zeolite crystal. It was shown that the pores and intersections in the zeolite can be accurately approximated as cylinders and cuboids with the specified dimensions. The maximum pore volume of the ZSM-5 zeolite was found to be  $0.227 \text{ cm}^3/\text{g}$ ; however, the complete volume cannot be utilized by water due to its molecule shape and van der Waal's radius. The radial distribution function of water in the zeolite was determined which showed three distinct peaks. In addition, it was shown that the molecular structure of water in the immediate proximity of a water molecule in water-saturated zeolite is similar to that of bulk water. Partial charge on zeolite atoms was found to be an important factor governing the transport of water in the pores. In order to corroborate simulation results with experiments, ZSM-5 zeolites were synthesized in-lab and pressure infiltration experiments were conducted. The average number of water molecules in the zeolite was obtained to be  $\sim 35.5 \pm 1.8$  per u.c., lower than that found in simulations. The reasons for the discrepancy were briefly discussed, and are further being examined in our ongoing research.

## ACKNOWLEDGMENTS

The authors would like to thank the King Fahd University of Petroleum and Minerals in Dhahran, Saudi Arabia, for funding the research reported in this paper through the Center for Clean Water and Clean Energy at MIT and KFUPM. The Intel Higher Education Grant is acknowledged for providing funds for computer workstations.



## REFERENCES

1. Cejka, J., *Introduction to zeolite science and practice*. 2007: p. 1058 p.
2. Li, L., et al., *Desalination by reverse osmosis using MFI zeolite membranes*. Journal of membrane science, 2004. **243**: p. 401-404.
3. Li, L., et al., *Counter ions on the reverse osmosis through MFI zeolite membranes: implications for produced water desalination*. Desalination, 2008. **228**: p. 217-225.
4. Lee, I., J.L. Buday, and H.K. Jeong,  *$\mu$ -Tiles and mortar approach: A simple technique for the facile fabrication of continuous b-oriented MFI silicalite-1 thin films*. Microporous and Mesoporous Materials, 2009.
5. Murad, S., K. Oder, and J. Lin, *Molecular simulation of osmosis, reverse osmosis, and electro-osmosis in aqueous and methanolic electrolyte solutions*. Molecular Physics, 1998. **95**(3): p. 401-408.
6. Murad, S.M. and J.C. Lin, *Using thin zeolite membranes and external electric fields to separate supercritical aqueous electrolyte solutions*. Ind. Eng. Chem. Res, 2002. **41**: p. 1076-1083.
7. Humplik, T., et al., *Nanostructured materials for water desalination*. Nanotechnology, 2011. **22**(29).
8. Li, D. and H.T. Wang, *Recent developments in reverse osmosis desalination membranes*. Journal of Materials Chemistry, 2010. **20**(22): p. 4551-4566.
9. Jeong, B.H., et al., *Interfacial polymerization of thin film nanocomposites: A new concept for reverse osmosis membranes*. Journal of membrane science, 2007. **294**(1-2): p. 1-7-1-7.
10. Trzpit, M., M. Soulard, and J. Patarin, *Water intrusion in mesoporous silicalite-1: An increase of the stored energy*. Microporous and Mesoporous Materials, 2009. **117**(3): p. 627-634.
11. Trzpit, M., et al., *The effect of local defects on water adsorption in silicalite-1 zeolite: a joint experimental and molecular simulation study*. Langmuir: the ACS journal of surfaces and colloids, 2007. **23**(20): p. 10131.
12. Cailliez, F., et al., *Thermodynamics of water intrusion in nanoporous hydrophobic solids*. Phys Chem Chem Phys, 2008. **10**(32): p. 4817-4826.
13. Eroshenko, V., et al., *Energetics: A new field of applications for hydrophobic zeolites*. Journal of the American Chemical Society, 2001. **123**(33): p. 8129-8130.
14. Hsu, C.Y., et al., *Rapid synthesis of MFI zeolite nanocrystals*. Journal of Physical Chemistry B, 2005. **109**(40): p. 18804-18814.
15. Zhao, J., et al., *Experimental Study on Energy Dissipation of Electrolytes in Nanopores*. Langmuir, 2009. **25**(21): p. 12687-12696.
16. Babeva, T., et al., *Optical properties of silica MFI doped acrylamide-based photopolymer*. Journal of Optics A, 2009.
17. Lu, W., et al., *Field-responsive ion transport in nanopores*. Appl Phys Lett, 2009. **94**(2): p. 023106.
18. Desbiens, N., A. Boutin, and I. Demachy, *Water condensation in hydrophobic silicalite-1 zeolite: A molecular simulation study*. J Phys Chem B, 2005. **109**(50): p. 24071-24076.
19. Van Der Spoel, D., et al., *GROMACS: fast, flexible, and free*. J Comput Chem, 2005. **26**(16): p. 1701-18.
20. Ch. Baerlocher, L.B.M. *Database of Zeolite Structures*. Available from: <http://www.iza-structure.org/databases/>.
21. Maijanen, A., E.G. Derouane, and J.B. Nagy, *FT-IR and solid-state NMR investigation of surface hydroxyl groups on dealuminated ZSM-5*. Applied Surface Science, 1994. **75**(1-4): p. 204-212.
22. Fritzsche, S., et al., *About the influence of lattice vibrations on the diffusion of methane in a cation-free LTA zeolite*. Chemical Physics Letters, 1998. **296**(3-4): p. 253-258.
23. Kopelevich, D., *Does lattice vibration drive diffusion in zeolites?* J. Chem. Phys., 2001. **114**(8): p. 3776.
24. Qiao, Y., L. Liu, and X. Chen, *Pressurized Liquid in Nanopores: A Modified Laplace-Young Equation*. Nano Letters, 2009. **9**(3): p. 984-988.